Lubrication Properties of a Brushlike Copolymer as a Function of the Amount of Solvent Absorbed within the Brush

Markus T. Müller,[†] Xiaoping Yan,[‡] Seunghwan Lee,[†] Scott S. Perry,[‡] and Nicholas D. Spencer*,[†]

Laboratory for Surface Science and Technology, Department of Materials, Swiss Federal Institute of Technology, ETH-Hönggerberg, Wolfgang-Pauli-Strasse 10, CH-8093 Zürich, Switzerland, and Department of Chemistry, University of Houston, Texas 77204-5003

Received January 25, 2005; Revised Manuscript Received May 2, 2005

ABSTRACT: The shear forces between poly(L-lysine)-*graft*-poly(ethylene glycol) (PLL-*g*-PEG)-modified SiO_2 tribopairs have been measured with colloidal-probe, lateral force microscopy (LFM) and related to the mass of solvent absorbed within the brushlike structure of immobilized PEG chains. The amount of solvent (per unit substrate area) absorbed within the tethered, brushlike polymer, referred to as areal solvation, Ψ, appears to be of importance in determining the lubrication properties of the tethered polymers. In this study, the degree of solvation was varied by choosing different solvents (aqueous buffer solution, methanol, ethanol, and 2-propanol) and was determined by a technique that combines the results of quartz crystal microbalance (QCM-D) experiments and optical waveguide lightmode spectroscopy (OWLS). The highest degree of solvation was measured for aqueous buffer solutions, and a progressive decrease in solvation of PLL-*g*-PEG was observed in moving from methanol to ethanol to 2-propanol. A concomitant increase in the measured shear force was observed with this decrease in solvation. The lubrication mechanism of the PLL-*g*-PEG-coated SiO_2 tribopair is discussed in terms of solvation and solvent quality and compared with the lubrication mechanism of the corresponding tribopair where only one surface is coated with the polymer brush.

Introduction

The lubrication properties of polymer "brushes", i.e., systems of polymers end-grafted to a flat surface, have been investigated in numerous experimental and theoretical studies.[1−14] Vanishingly low friction forces have been reported for solid surfaces bearing polymer brushes under good solvent conditions and in the low-contact-pressure regime of the surface forces apparatus (SFA).[1] When brushlike polymers are brought into contact under good solvent conditions, long-ranged repulsive forces of osmotic origin act to keep the surfaces apart and entropic effects restrict mutual interpenetration of opposing polymer chains to a narrow interfacial zone, thus maintaining a highly fluid layer at the interface between them.[4,7,8,11] The effective viscosity in that zone differs only slightly from the solvent viscosity prevailing outside of the contact area. Hence, in the low-pressure regime of the SFA, the force required to maintain sliding is extraordinarily low and corresponds solely to the viscous drag of the polymer chain ends in the narrow interpenetration zone.[4] However, under the high-pressure regime of some 100 MPa, exerted by a colloidal-probe lateral force microscope (LFM), compression of the brush becomes more significant and the resistance to shear increases somewhat; nevertheless, friction still remains low.[15]

In this work, poly(ethylene glycol) brushes were formed from the comblike graft copolymer poly(L-lysine)-*graft*-poly(ethylene glycol) (PLL-*g*-PEG). This was synthesized by covalently linking PEG to a cationic poly(L-lysine) backbone. The structure of PLL-*g*-PEG is depicted in Figure 1. It consists of PEG chains that are attached to a PLL backbone, which is positively charged at pH

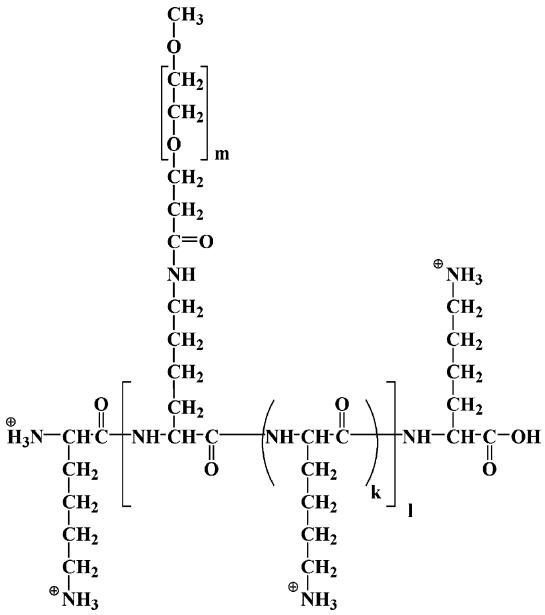

Figure 1. Structure of PLL-*g*-PEG.

≤ 10 due to protonation of the primary amine groups. In aqueous buffer solution, the PLL backbone readily adsorbs, for electrostatic reasons, onto a negatively charged surface, such as an oxide, forcing the PEG side chains into a dense, brushlike structure as depicted schematically in Figure 2A. Replacement of the good solvent (e.g., aqueous buffer solution) for a solvent of inferior quality (e.g., organic solvents) causes a contraction of the PEG brush to a more random, coillike conformation (Figure 2B).[16,17]

PEG has been extensively investigated for application in a wide array of biomedical devices, since immobilization of PEG onto surfaces has long been known to

[†] Swiss Federal Institute of Technology.
[‡] University of Houston.

10.1021/ma0501545 CCC: $30.25
Published on Web 06/04/2005

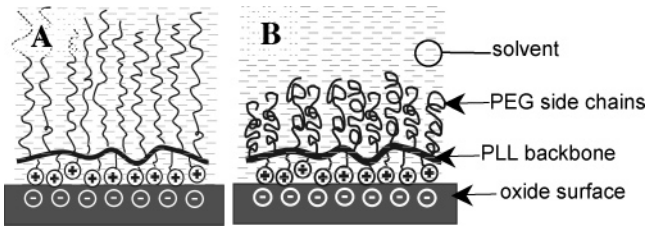

Figure 2. Schematic diagram of PLL-*g*-PEG adsorbed onto a negatively charged surface in (A) good solvent and (B) bad solvent.

decrease protein adsorption.[18−23] Very recently, PLL-*g*-PEG has also attracted interest in the field of tribology. Both macro- and nanoscale tribological studies have shown a significant reduction of interfacial friction between two PLL-*g*-PEG-coated oxide surfaces in an aqueous environment.[15,24,25]

The present study aims to understand the influence of solvent quality on the molecular-level friction mechanism of tethered, brushlike polymers. It involves complementary adsorption studies of PLL-*g*-PEG by means of optical waveguide lightmode spectroscopy (OWLS) and quartz crystal microbalance with dissipation (QCM-D) as well as friction studies performed on the nanoscale using colloidal-probe lateral force microscopy (LFM). The adsorbed mass measured by QCM-D includes a contribution from solvent molecules absorbed within the surface-bound polymer film.[23,26,27] This is in contrast to optical techniques, such as OWLS, which are sensitive only to the "dry mass" of a polymer adsorbed onto the surface of the waveguide.[28,29] By subtracting the "dry mass", derived from OWLS measurements, from the "wet mass", derived from QCM-D measurements, it is therefore possible to determine the mass of the solvent per unit substrate area absorbed in the brushlike structure of PLL-*g*-PEG, expressed as areal solvation, Ψ. Areal solvation was varied by choosing solvents (aqueous buffer solution, methanol, ethanol, and 2-propanol) of different quality with respect to the PEG brush. The solvents were characterized in terms of the three-component Hansen solubility parameters,[30] and these values were compared with measured areal solvation of the PEG brush.

The amount of solvent absorbed within a polymer brush is of great significance because it is regarded as a key parameter in determining the lubrication properties of brushlike polymers.[11,12] In this study we examined the relation between areal solvation of an unperturbed PLL-*g*-PEG-bearing SiO_2 surface and the force needed to shear two PLL-*g*-PEG-bearing SiO_2 surfaces past each other by the use of colloidal-probe LFM in liquid. The molecular friction mechanism is discussed in the context of solvation and on the basis of experiments performed on PLL-*g*-PEG-bearing tribopairs and on bare silica sliding against a flat PLL-*g*-PEG-bearing silica counter surface.

Materials and Methods

Synthesis of Poly(L-lysine)-*graft*-poly(ethylene glycol) (PLL-*g*-PEG). The synthesis of poly(L-lysine)-*graft*-poly(ethylene glycol) (PLL-*g*-PEG) molecules has been previously described.[20,31] PLL−HBr (Fluka, Switzerland) was dissolved at a concentration of 100 mM in SBB (sodium borate buffer solution, 50 mM) adjusted to pH 8.5. The solution was filter-sterilized (0.22 μm pore size filter). For the grafting of PEG onto PLL, the *N*-hydroxysuccinimidyl ester of methoxypoly(ethylene glycol) propionic acid (mPEG-SPA, Nektar, Huntsville, AL) was added to PLL−HBr solution. The reaction was allowed to proceed for 6 h at room temperature, after which the reaction mixture was dialyzed (Spectra-Por, mol wt cutoff size 6−8 kDa, Spectrum, Houston, TX) for 48 h against deionized water. The PEG graft ratio y, the number of lysine monomers per PEG chain, was determined using ^{1}H NMR. The product was freeze-dried and stored in powder form at −20 °C. The nomenclature of these polymers takes the form of PLL(x)-*g*[y]-PEG(z) and signifies that the graft copolymer has a PLL backbone derived from PLL−HBr of molecular weight x kDa, a graft ratio y = number of lysine units/PEG side chain, and PEG side chains of molecular weight z kDa. In the present study, we used PLL(20)-*g*[3.5]-PEG(5): a PLL backbone of molecular weight 12 kDa, corresponding to 20 kDa PLL-HBr, was used for synthesis, and the polydispersity was M_w/M_n = 1.2. The grafting ratio was g = 3.5, and the PEG side chains were of molecular weight 5 kDa with a polydispersity of M_w/M_n = 1.1. The structure of the PLL-*g*-PEG polymer is shown in Figure 1, and the adsorption of PLL-*g*-PEG onto a negatively charged oxide surface is depicted in Figure 2.

Surface Preparation. PLL(20)-*g*[3.5]-PEG(5) adlayers were prepared by immersion of SiO_2 films into an aqueous buffer solution of the polymer. The films were sputter-coated onto quartz crystals for QCM-D or onto optical waveguides for OWLS. For LFM measurements, thermally oxidized Si (100) wafers and colloidal SiO_2 probes (diameter = 5.1 μm) were employed. Prior to immobilization of the polymer onto the surface, the oxidized Si (100) wafers and SiO_2 colloidal probe were treated by the following procedure: sonication in toluene for 2 min and then in 2-propanol for 10 min followed by extensive rinsing with ultrapure water (18.3 MΩ cm) (EM Science, Gibbstown, NJ), drying in a nitrogen flow, and exposure to an oxygen plasma PDC-32G (Harrick Scientific Corp., Ossining, NY) for 2 min (10 s in the case of the colloidal SiO_2 probes). The power applied to the rf coil of the plasma cleaner was set to 18 W. The oxidized substrate and the colloidal probe were immediately transferred to a 0.25 mg/mL solution of PLL(20)-*g*[3.5]-PEG(5) in 10 mM HEPES (4-[2-hydroxyethyl]piperazine-1-[2-ethanesulfonic acid], pH 7.4) buffer solution for 30 min and subsequently rinsed with polymer-free aqueous HEPES buffer solution to remove unbound PLL-*g*-PEG from the surface. The SiO_2 sputter-coated quartz crystal sensors and the optical waveguides were treated in a manner similar to the Si (100) wafers, but the plasma cleaning was reduced to 10 s in order to prevent damage to the thin SiO_2 coating. In the case of OWLS and QCM-D, the polymer was allowed to adsorb onto the sample directly in the liquid cell of the analytical devices.

Optical Waveguide Lightmode Spectroscopy (OWLS). Optical waveguide lightmode spectroscopy (OWLS) was carried out on a BIOS-I instrument (ASI AG, Zürich, Switzerland) using a Kalrez (Dupont, Wilmington, DE) flow-through cell with a volume of 16 μL. The waveguide chips used for OWLS measurements (MicroVacuum Ltd. Budapest, Hungary) consisted of a 1 mm thick glass substrate and a 200 nm thick $Si_{0.75}Ti_{0.25}O_2$ waveguiding layer at the surface. A silica layer (ca. 12 nm) was sputter-coated on top of the waveguiding layer in a Leybold dc-magnetron Z600 sputtering unit. The coating conditions and the principles of OWLS investigations have been described in detail elsewhere.[28,29] Briefly, in optical waveguide lightmode spectroscopy, the adsorbed mass is calculated from the change of the refractive index in the vicinity of the surface upon adsorption of molecules from solution. The refractive index is a linear function of the concentration over a wide range, and thus the absolute amount of the adsorbed molecules can be determined using de Feijter's formula.[32] A refractive index increment (dn/dc) value of 0.134 cm^3/g for PLL(20)-*g*[3.5]-PEG(5) was derived from a linear interpolation between 0.13 cm^3/g (pure PEG) and 0.18 cm^3/g (pure PLL). It is important to note that the surface-adsorbed areal mass density determined by OWLS is regarded as a "dry areal mass density" due to the fact that solvent molecules coupled to the adsorbate will not contribute to a change in the refractive index and thus do not contribute to the detected

adsorbate mass. The reported dry areal mass density, m_{dry}, represents the average of three individual experiments.

Quartz Crystal Microbalance with Dissipation (QCM-D). All QCM-D measurements were performed with a commercial quartz crystal microbalance with dissipation monitoring from Q-Sense, Gothenburg, Sweden.[33] The instrument was equipped with a home-built laminar flow cell with a glass window that allows visual monitoring of the injection and exchange of the liquids. The sensor crystals used in the measurements were 5 MHz AT-cut quartz, sputter-coated with SiO_2 (Q-Sense). All measurements were recorded at four different frequencies (5, 15, 25, 35 MHz). The QCM-D liquid chamber was temperature-stabilized to 25 ± 0.02 °C. The QCM-D response, i.e. changes in both resonant frequency, Δf_0, and the dissipation factor, ΔD, at different overtones, is, in contrast to OWLS, sensitive to viscoelastic properties and density of any mass coupled to the mechanical oscillation of the quartz crystal. In our case, the adsorbed mass consists of the copolymer, PLL-*g*-PEG, along with solvent molecules coupled to the polymer. The positively charged PLL backbone is strongly attached to the negatively charged SiO_2 sensor surface whereas, depending on the solvent quality, the PEG side chains form a solvated brushlike structure, extending into the liquid phase, thereby incorporating solvent molecules within the brush (see schematic representation in Figure 2). These absorbed solvent molecules may be loosely associated (i.e., hydrodynamically) or strongly attracted (e.g., via hydrogen bonding) to the brush but do not behave like bulk liquid above the film when probed by the crystal's oscillation. Hence, it is important to note that the mass sensed by QCM-D is the mass of polymer plus the mass of absorbed solvent molecules and is referred to as wet mass, m_{wet}, in contrast to the dry mass, m_{dry}, obtained by OWLS.[34]

In QCM-D, the change in resonance frequency is often directly related to the mass of the adsorbed layer according to the Sauerbrey equation (eq 1):[35]

$$m_{wet(Sauerbrey)} = -C\frac{\Delta f}{n} \quad (1)$$

where $m_{wet(Sauerbrey)}$ is the adsorbed mass, C is a constant characteristic of the crystal, Δf is the change in frequency, and n is the shear wavenumber. However, the Sauerbrey equation holds strictly only in a vacuum and gaseous environments.[36] Thus, in this study, we used a Voigt-based model (software: Q-tools, version 2.0.1) where the adsorbed layer is represented by a homogeneous viscoelastic film characterized by a shear viscosity, η_{shear}, a shear modulus, E_{shear}, and a film thickness, h_{film}.[36−38] The input parameters include the viscosity and the density of the solvent and the density of the polymer film, ρ_{film}. While the viscosity and density of the solvents used in the present study are well-known, ρ_{film} remains unknown. However, ρ_{film} can be approximated fairly well by combining the mass fraction of its contributory terms, $\rho_{solvent}$ and $\rho_{polymer}$ (eq 2). The relative weighting of the two terms, $\rho_{solvent}$ and $\rho_{polymer}$, can be calculated using both m_{dry} and m_{wet}. While m_{dry} is known from OWLS experiments, m_{wet} must be estimated by applying eq 1 using the Δf obtained by QCM-D experiments.

$$\rho_{film} = \frac{m_{wet(Sauerbrey)} - m_{dry}}{m_{wet(Sauerbrey)}}\rho_{solvent} + \frac{m_{dry}}{m_{wet(Sauerbrey)}}\rho_{polymer} \quad (2)$$

where $m_{wet(Sauerbrey)}$ is the mass derived from the Sauerbrey equation. $\rho_{polymer}$ stands for the density of PLL-*g*-PEG (≈1 g/cm^3) and $\rho_{solvent}$ for the densities of the liquids, being $\rho_{HEPES} = 1.0$, $\rho_{methanol} = 0.791$, $\rho_{ethanol} = 0.787$, and $\rho_{2-propanol} = 0.786$ g/cm^3 for aqueous HEPES buffer solution, methanol, ethanol, and 2-propanol, respectively.[39] By multiplying the layer thickness h_{film}, obtained by the Voigt-based model, by ρ_{film}, we obtain the wet areal mass density, m_{wet}, which in our case is some 5−10% higher than the wet mass density, $m_{wet(Sauerbrey)}$, derived from the Sauerbrey equation. In agreement with Larson et al.,[38] we observed that, unlike h_{film}, m_{wet} does not depend on the choice of the input parameter ρ_{film}. The value of m_{wet} is preserved as it results from the multiplication of h_{film} and the input parameter ρ_{film} which is obtained from eq 2. The reported wet mass density, m_{wet}, represents the average of three individual experiments performed on the same quartz crystal.

Atomic Force Microscopy. A home-built atomic force microscope was used to probe frictional forces of the polymer-modified SiO_2 substrates in liquid environments. The microscope was equipped with a liquid cell/tip holder (Digital Instruments, Santa Barbara, CA) and controlled by SPM 1000 electronics and SPM 32 software (RHK Technology, Inc., Troy, MI). A silica microsphere (diameter = 5.1 μm), attached to an AFM cantilever (Novascan Technologies, Ames, IA), was used as the counterface to the polymer-modified SiO_2 surface. Kinetic friction data were acquired by monitoring the lateral deflection of the cantilever as a function of position across the sample surface while sliding. While the sample was rastered in a line-scan mode, the load was first increased and then decreased. During this procedure, frictional forces and normal forces were measured simultaneously at a scan speed of ≈1.4 μm/s over a distance of 0.1 μm. The reported frictional data represent the average of at least six results obtained at different locations as a function of decreasing load across the surface. Normal loads were limited to ≈35 nN in order to avoid wear of the tip and surface, which would invalidate the comparison of frictional data. AFM measurements were carried out in the sequence of aqueous HEPES buffer solution, methanol, ethanol, and 2-propanol. The composition of the liquid environment encompassing the tip−sample interface was controlled by transferring aliquots of solvents in and out of the liquid cell through the use of two 5 mL syringes.

In the reported AFM measurements, normal loads have been calibrated directly from the reported spring constant of AFM cantilever (0.58 N/m), while the friction forces have been calibrated through an improved wedge calibration method. Briefly, the force calibration was experimentally carried out by sliding the tip across a silicon grating surface containing two known slopes (TGG01, MikroMasch, Narva mnt 13, 10151 Tallinn, Estonia) as a function of applied load. More details of this calibration method have been reported elsewhere.[40,41]

Results

Comparative Adsorption Measurements Using QCM-D and OWLS. In a QCM-D experiment the resonance frequency, f_0, and the dissipation factor, D, of a single quartz crystal were measured first in one of the organic solvents (methanol, ethanol, or 2-propanol) and subsequently in aqueous HEPES buffer solution to set baselines. After recording the baselines, the polymer-free aqueous HEPES buffer solution was replaced by PLL(20)-*g*[3.5]-PEG(5)-containing aqueous HEPES buffer solution (0.25 mg/mL). After adsorption for 30 min, the liquid cell was rinsed with polymer-free aqueous HEPES buffer solution, and f_0 and D were recorded. Subsequently, the aqueous HEPES buffer solution was exchanged by one of the organic solvents, and both f_0 and D were recorded again. Note that PLL-*g*-PEG was allowed to adsorb only from aqueous HEPES buffer solution. To ascertain that no surface-bound polymer desorbed due to the solvent exchange, the organic solvent was once again replaced by aqueous HEPES buffer solution. The shift in both f_0 and D upon this control measurement was highly reproducible with Δf_0 and ΔD measured for the solvent exchange directly after the polymer adsorption showing that no surface-bound polymer was lost during solvent exchange. The raw data from a typical QCM-D measurement for the HEPES−methanol system are displayed in Figure 3. The difference in both f_0 and D before and after polymer adsorption is a measure of the mass of the adsorbate in the corresponding solvent and is converted to a mass per

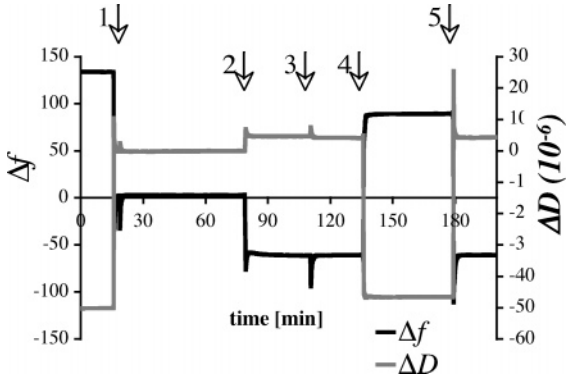

Figure 3. Changes in the normalized third overtone resonance frequency, Δf (black line), and dissipation, ΔD (gray line), during adsorption of PLL(20)-*g*[3.5]-PEG(5) onto a SiO_2 sputter-coated surface for the HEPES−methanol system (polymer injection at arrow number 2). Before injection of the polymer the baseline of the SiO_2-coated quartz crystal was measured in methanol and subsequently in HEPES buffer solution. The exchange of methanol for HEPES buffer solution is indicated by the arrow number 1. The measurement chamber was rinsed with polymer-free aqueous HEPES buffer solution 30 min after polymer injection (arrow number 3). Subsequently, the aqueous HEPES buffer solution was replaced by methanol, and the resonance frequency f_0 and the dissipation factor D were measured again (arrow number 4). The reproducibility of the Δf_0 and ΔD shifts upon solvent changes was tested by replacing methanol by aqueous HEPES buffer solution (arrow number 5). This measurement protocol for the methanol solvent system was repeated and applied to the other two solvent systems, ethanol and 2-propanol.

unit area using a Voigt-based model described in the Experimental Section. The obtained masses, referred to as wet mass, m_{wet}, are $m_{wet(HEPES)} = 1240.6$ ng/cm^2, $m_{wet(methanol)} = 876$ ng/cm^2, $m_{wet(ethanol)} = 637$ ng/cm^2, and $m_{wet(2-propanol)} = 402$ ng/cm^2 for aqueous HEPES buffer solution, methanol, ethanol, and 2-propanol, respectively. To obtain the dry mass of the surface adsorbed copolymer, we utilized *in situ* OWLS. The advantage of using OWLS instead of QCM-D for determining the adsorbed mass is that OWLS is an optical technique, which allows the quantification of the "dry" polymer mass in a liquid environment. The average dry mass value of PLL(20)-*g*[3.4]-PEG(5) adsorbed on a SiO_2 coated waveguide is $m_{dry} = 198$ ng/cm^2. By subtracting the dry mass from the wet mass, the solvent mass per unit substrate area, or areal solvation, Ψ, is obtained. It was found that the solvation is highest for aqueous HEPES buffer solution ($\Psi = 1043$ ng/cm^2) and decreases in the order of methanol ($\Psi = 678$ ng/cm^2), ethanol ($\Psi = 439$ ng/cm^2), and 2-propanol ($\Psi = 204$ ng/cm^2). From the experimental results for m_{dry} and m_{wet} it is feasible to calculate the number of solvent molecules per EG monomer averaged over the cross section of the PEG brush, $\Lambda_{sol/EG}$, by applying the following equations:

$$\Sigma_{sol} = \frac{N_A(m_{wet} - m_{dry})}{Mw_{sol}} \tag{2}$$

$$\Sigma_{EG} = \frac{Mw_{PLL}Mw_{PEG}m_{dry}}{N_A Mw_{EG}Mw_{LL}g\left(Mw_{PLL} + \frac{Mw_{PLL}Mw_{PEG}}{Mw_{LL}g}\right)} \tag{3}$$

$$\Lambda_{sol/EG} = \frac{\Sigma_{sol}}{\Sigma_{EG}} \tag{4}$$

where Σ_{sol} and Σ_{EG} are the areal density of the solvent molecules and ethylene glycol monomer units, EG, respectively, N_a is the Avogadro constant, Mw_{sol} is the molecular weight of the solvent, Mw_{PLL} is the molecular weight of the PLL backbone, Mw_{LL} is the molecular weight of a L-lysine monomer unit, Mw_{PEG} is the molecular weight of a PEG side chain, Mw_{EG} is the molecular weight of an ethylene glycol monomer unit, and g is the grafting ratio of the copolymer PLL-*g*-PEG. The calculated average ratio of EG monomers to solvent molecules of PLL-*g*-PEG immersed in HEPES aqueous buffer solutions is $\Lambda_{water/EG} = 14$, in methanol $\Lambda_{methanol/EG} = 5.1$, in ethanol $\Lambda_{ethanol/EG} = 2.3$, and in 2-propanol $\Lambda_{2-propanol/EG} = 0.8$.

Another technique that was used to estimate the solvent content and the number of solvent molecules per EG monomers of PLL-*g*-PEG coatings was recently developed by Pasche et al. and involves colloidal-probe AFM surface force measurements.[42] The main assumption made in this technique is that the unperturbed PEG layer is compressed by the colloidal probe from a fully solvated state to a solvent-free, dry state. Thus, the decrease in the layer thickness upon compression is likely to reflect the amount of solvent absorbed within the polymer brush. The results of that study are in reasonable agreement with the findings of the present work.

Table 1 provides an overview of the results of the comparative adsorption measurements using QCM-D and OWLS together with the coefficients of friction, which will be discussed below.

Solvent Characteristics. In an attempt to rationalize the effect of solvent characteristics on solvation, we make use of the three-component Hansen solubility parameter model.[30,43] These solubility parameters are commonly used in polymer chemistry to predict the solubility of a polymer in a solvent.[44] The Hansen solubility parameters are defined in terms of the cohesive energy density that relates to the amount of energy required to vaporize 1 mol of the solvent.

$$\delta = \left(\frac{-E}{V}\right)^{0.5} \tag{5}$$

where $-E$ is the internal energy change of vaporization and V is the molar volume of the solvent at the temperature of vaporization. Each solvent is characterized by a set of three parameters δ (Hansen solubility parameters, HSP) designated by subscripts d (dispersion), p (polar), and h (hydrogen bonding), according to the nature of the intermolecular cohesion energy they reflect. Total cohesion energy, $-E$, is then the sum of the individual energies that comprise it.

$$-E = -E_d - E_p - E_h \tag{6}$$

Dividing this by the molar volume, V, gives the total Hansen solubility parameter δ_0 (eq 7).

$$\delta_0^2 = -\frac{E}{V} = -\frac{E_d}{V} - \frac{E_p}{V} - \frac{E_h}{V} \tag{7}$$

This parameter can also be stated in a form in which the individual terms refer to the dispersion, polar, and hydrogen-bonding parameters δ_d, δ_p, and δ_h, respectively (eq 8).

$$\delta_0^2 = \delta_d^2 + \delta_p^2 + \delta_h^2 \tag{8}$$

Table 1. Average Values (± Standard Deviation) for PLL(20)-*g*[3.5]-PEG(5), Adsorbed on a Silica Substrate Surface, of the Wet Mass Density, m_{wet}, the Dry Mass Density, m_{dry}, the Solvation, Ψ, the Number of Solvent Molecules per EG Monomer Averaged over the Cross Section of the PEG Brush, $\Lambda_{sol/EG}$, and the Coefficient of Friction for Symmetric (Silicon Wafer and Colloidal Probe Coated with PLL-*g*-PEG), and Asymmetric (Silicon Wafer Coated with PLL-*g*-PEG, Colloidal Probe Uncoated) Tribopairs

polymer−solvent system	h_{film} [nm]	m_{wet} [ng/cm^2]	m_{dry} [ng/cm^2]	ψ [ng/cm^2]	$\Lambda_{sol/EG}$	μ (symmetric)	μ (asymmetric)
HEPES	12.4	1240.6 ± 62.9	197.8 ± 12.2	1042.7 ± 61.7	14	0.035 ± 0.001	0.220 ± 0.008
methanol	10.5	875.8 ± 52.5		678.0 ± 51.0	5.1	0.081 ± 0.001	0.306 ± 0.007
ethanol	7.5	636.7 ± 43.3		438.8 ± 41.6	2.3	0.159 ± 0.013	0.450 ± 0.01
2-propanol	4.6	401.5 ± 21.9		203.7 ± 18.2	0.8	0.321 ± 0.002	0.572 ± 0.007

Table 2. Hansen Solubility Parameters[30] (δ_0 = Total Hansen Solubility Parameter, δ_d = Dispersion Parameter, δ_p = Polar Parameter, δ_h = Hydrogen-Bonding Parameter)

Hansen no.	solvent	ψ [ng/cm^2]	δ_0 [MPa$^{1/2}$]	δ_d [MPa$^{1/2}$]	δ_p [MPa$^{1/2}$]	δ_h [MPa$^{1/2}$]
696	water	1042.7 ± 61.7	47.9	15.5	16	42.4
570	methanol	678.0 ± 51.0	29.7	15.1	12.3	22.3
325	ethanol	438.8 ± 41.6	26.6	15.8	8.8	19.4
456	2-propanol	203.7 ± 18.2	23.5	15.8	6.1	16.9

Table 2 summarizes the values of solvation of the different solvent/PLL-*g*-PEG systems as a function of the total Hansen solubility parameters as well as a function of the single Hansen solubility parameters of the solvents, while Figure 4 represents these data in a graphical format. The total solubility parameter of the solvents decreases in the order water ($\delta_0 = 47.9$ MPa$^{1/2}$), methanol ($\delta_0 = 29.7$ MPa$^{1/2}$), ethanol ($\delta_0 = 26.6$ MPa$^{1/2}$), and 2-propanol ($\delta_0 = 23.5$ MPa$^{1/2}$). Solvation decreases in the same order; thus, a strong correlation between the Hansen solubility parameters and the measured solvation of the PEG brush is observed in Figure 4A. The values of the dispersion parameter of the solvents all fall within the very narrow range of 15.1 MPa$^{1/2}$ < δ_d < 15.8 MPa$^{1/2}$, and no systematic dependency between the dispersion parameter and solvation is observed in Figure 4B. However, when the solvation is plotted as a function of either the polar solubility parameter (Figure 4C) or the hydrogen-bonding solubility parameter (Figure 4D), a strong positive correlation is observed.

Frictional Properties of PLL-*g*-PEG in Different Solvents Using LFM. Figure 5 shows friction vs load measurements for "symmetric" (both the silicon wafer and the colloidal probe are coated with PLL-*g*-PEG) and "asymmetric" (only the silicon wafer is coated with PLL-*g*-PEG and the colloidal probe remained uncoated) interfaces under the different solvents (aqueous HEPES buffer solution, methanol, ethanol, 2-propanol). In both cases all friction curves show a linear dependence on load and go through the origin, indicating that the interfacial contact between colloidal probe and substrate is of a nonadhesive nature. Further, a clear dependence of the friction force on the type of solvent is observed over the entire range of loads investigated in this study. The slopes of the friction−load plots for both tribosystems decrease steeply in the order 2-propanol, ethanol, methanol, and aqueous HEPES buffer solution. Sliding contact of the asymmetric tribosystem showed higher friction forces than the symmetric case throughout the study. Table 1 lists the coefficients of friction, μ, obtained from the linear portion of the friction vs load plots, whereas in Figure 6, the coefficients of friction are plotted against areal solvation, Ψ. Both tribosystems, asymmetric and symmetric, experience a significant increase in the coefficient of friction with decreasing solvation. Interestingly, the shapes of the two plots are very similar. The absence of a qualitative difference for

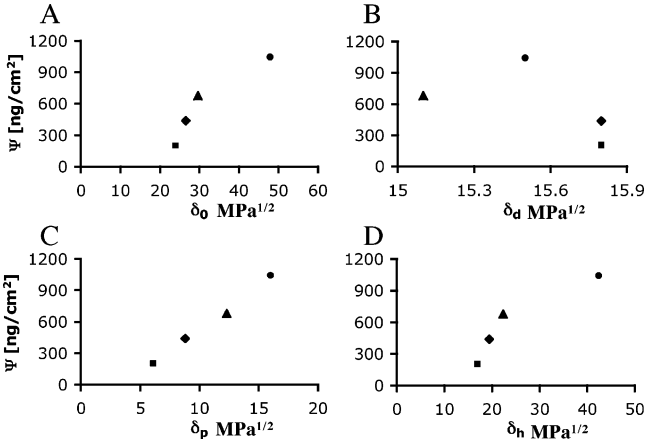

Figure 4. Effect of the total, δ_0, and the individual Hansen solubility parameters, δ_d, δ_p, δ_h, on the solvation, Ψ, of the PEG side chains. The study investigated the following solvents: ●, water; ▲, methanol; ◆, ethanol; ■, 2-propanol.

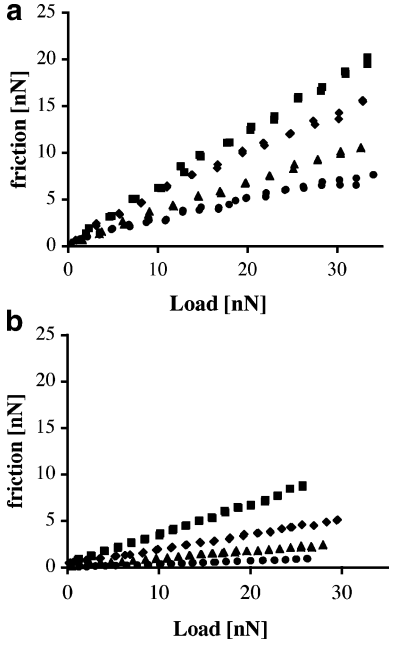

Figure 5. (●) Water, (▲) methanol, (◆) ethanol, and (■) 2-propanol. Interfacial friction measured as a function of decreasing load for the contact of (a) a bare and (b) a PLL-(20)-*g*[3.5]-PEG(5)-modified SiO_2 colloidal LFM-probe (diameter = 5.1 μm) and SiO_2 substrates coated with PLL(20)-*g*[3.5]-PEG(5). A single colloidal LFM probe was employed throughout the series of measurements.

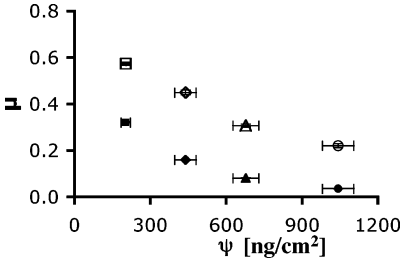

Figure 6. Coefficient of friction, μ, vs solvation, Ψ, for both asymmetric (open symbols) and symmetric (filled symbols) PLL(20)-*g*[3.5]-PEG(5) coated tribointerfaces (●, water; ▲, methanol; ◆, ethanol; ■, 2-propanol). Coefficients of friction were derived from a linear regression of the friction−load plots shown in Figure 5 and represent the mean values of three experiments (± standard deviation).

the two cases (symmetric and asymmetric) suggests that the molecular friction mechanism is not substantially different for these tribopairs.

Discussion

Previous tribological studies on PLL-*g*-PEG bearing tribopairs revealed a significant reduction of interfacial friction in an aqueous environment on both the macro- and the nanoscale.[15,24,25] The excellent lubrication properties of PLL-*g*-PEG have been ascribed to its distinctive adsorption behavior: the positively charged amino groups of the PLL backbone are electrostatically attracted to negatively charged oxide surfaces, forcing the PEG chains into a dense, brushlike structure that is highly solvated, storing a significant amount of solvent, when under good solvent conditions (Figure 2). To elucidate the relationship between solvent quality, conformation of the PEG brush, and the lubrication properties, we have quantified the amount of solvent absorbed in the PEG brush of surface-bound PLL-*g*-PEG in different solvents that vary in solvent quality with respect to PEG.

The wet mass obtained by QCM-D and the dry mass obtained by OWLS for PLL-*g*-PEG adsorbed from aqueous HEPES buffer solution on a flat SiO_2 substrate surface are $m_{wet} = 1241$ ng/cm^2 and $m_{dry} = 198$ ng/cm^2, respectively, resulting in a solvation of $\Psi = 1043$ ng/cm^2. This means that in the case where the PLL-*g*-PEG-bearing interface is immersed in aqueous HEPES buffer solutions, the mass of the hydrated PLL-*g*-PEG adlayer is more than 80% aqueous buffer solution and less than 20% polymer. However, in the case where the aqueous HEPES buffer solution is exchanged for an organic solvent, the mass of solvent molecules absorbed in the PEG brush reduces in the order $\Psi = 678$ ng/cm^2 for methanol, $\Psi = 438$ ng/cm^2 for ethanol, and $\Psi = 203$ ng/cm^2 for 2-propanol. It is important to note that the PLL-*g*-PEG layers were only adsorbed from pure aqueous HEPES buffer solution, and in the case of the organic solvents, a repeated exchange of the aqueous HEPES buffer solution for one of the organic solvents was carried out. To ensure a complete exchange of the solvent, the liquid cell was purged with an excess amount of liquid. We conclude that the quality of solvent, with respect to the PEG brush, decreases in the order aqueous HEPES buffer solution, methanol, ethanol, and 2-propanol.

The friction force measurements were performed in two different configurations: asymmetric, where only the flat substrate surface was coated by PLL-*g*-PEG and the colloidal probe of the LFM remains bare, and symmetric, where both surfaces were coated by PLL-*g*-PEG. As shown in Figure 5, all the friction−load plots obtained in this study show an Amontons-type behavior, and thus the coefficient of friction can be expressed through linear regressions of the friction−load plots. The coefficients of friction for all the measurements performed in this study are listed in Table 1. Raviv et al.[45] have reported on the properties and interactions of end-functionalized PEG ($M_w = 3400$ Da) layers physically grafted on mica and measured in aqueous solution by means of surface force apparatus (SFA). For the case of a symmetrically coated tribopair in the present study, the measured coefficient of friction, $\mu = 0.035 \pm 0.001$, is comparable to the value reported by Raviv et al.,[45] $\mu = 0.03$.

As expected, the coefficient of friction for both asymmetric and symmetric interfaces showed a clear dependence on the type of solvent. For both types of interface, the coefficient of friction increases in the same order as the solvent quality decreases: aqueous HEPES buffer solution, methanol, ethanol, and 2-propanol.

A comparison of the coefficient of friction with the amount of solvent molecules absorbed in the brushlike structure of PLL-*g*-PEG is shown in Figure 6. A strong correlation between coefficient of friction and solvation is observed for both symmetric and asymmetric tribointerfaces; i.e., the higher the solvation, the lower the coefficient of friction.

It is generally accepted that PEG has a strong tendency to hydrogen bond with surrounding water molecules, thus forming PEG−water complexes with a composition of approximately three water molecules directly associated with each EG monomer unit.[46] However, a closer examination of the experimental results of this study reveals that in aqueous HEPES buffer solution every EG monomer of the surface-bound PLL-*g*-PEG brush is, on the average over the whole interface of the polymer brush layer, surrounded by 14 water molecules, $\Lambda_{water/EG} = 14$. Thus, it can be concluded that, in addition to the three hydrogen-bonded water molecules, on average there exist another 11 water molecules per EG monomer within the brush structure immersed in aqueous HEPES solution. In comparison, the ratio of EG monomers to solvent molecules in methanol, ethanol, and 2-propanol is approximately $\Lambda_{methanol/EG} = 5.1$, $\Lambda_{ethanol/EG} = 2.3$, and $\Lambda_{2-propanol/EG} = 0.8$, respectively. However, it is not likely that hydrogen-bonded water molecules will easily be removed by a solvent exchange. Thus, in the case of the organic solvents, the ratio of EG monomers to solvent molecules, stated above, represents an overestimation by the fact that a small portion of water molecules will possibly remain in the brush structure following the exchange of the solvent. From the analysis of the solvents in terms of the Hansen solubility parameters, a fair correlation of the brush solvation with the total solubility parameter is observed in Figure 4. A detailed analysis of the different solubility parameters as a function of solvation reveals that there is no correlation between solvation and the dispersion parameter (Figure 4B). However, when solvation is plotted as a function of either the polar or the hydrogen-bonding interaction parameters, a strong correlation is observed (Figure 4C,D). The ability of the PEG brush to absorb solvent molecules from the bulk solution increases significantly with the increase of both the solvent's polar and hydrogen-bonding interaction parameters. This is not

unexpected; the formation of structures between the solvent molecules and the monomer units of PEG is progressively less pronounced in the case of the organic solvents because the organic solvents show a significantly weaker ability to form either dipole−dipole interactions or hydrogen bonds, when compared to water. Thus, the interactions of the EG/EG monomer units become relatively more attractive with the deterioration of the solvent quality, and the remaining organic solvent molecules absorbed in the structure of the PEG chains experience a progressively smaller retaining force compared to the water molecules, as hydrogen-bonding and polar interactions decrease. As a result, solvent molecules are squeezed out more easily when the PLL-*g*-PEG interface comes under compression under poor solvent conditions. The case of a PLL-*g*-PEG-bearing tribopair sliding in a solvent of inferior quality, therefore, differs significantly from that of a PLL-*g*-PEG bearing tribopair sliding in good solvents as both long-ranged repulsive forces of osmotic origin and the entropic effects restricting mutual interpenetration are reduced under conditions of poor solvent quality. This leads to a less fluid and less mobile interface where more energy is dissipated during sliding motion, resulting in a higher coefficient of friction for brush-bearing tribopairs sliding in solvents of inferior quality.

Comparing the results of the friction force measurements for the two different tribogeometries, asymmetric and symmetric, it is important to note that the sliding contact of the asymmetric tribosystem shows significantly higher friction forces compared to that of the symmetric tribosystem throughout this work. However, the dependence of the coefficient of friction on areal solvation for the asymmetric case mirrors that of the symmetric interface (Figure 6). This behavior strongly suggests that the molecular friction mechanism is not intrinsically different for the two different tribointerfaces although the contact zone of the asymmetric interface differs from that of the symmetric interface in a number of important aspects.[10] In the former case, the polymer brush encounters the rigid surface of the SiO_2 colloidal probe of the LFM, whereas in the latter case, surface-bound PLL-*g*-PEG contacts an opposing PLL-*g*-PEG brush layer. In both cases, attractive forces must also be considered within the contact zone of the two opposing tribopairs due to potential bridging forces in the asymmetric case and due to both entanglement and bridging forces of opposing PEG chains in the symmetric case.[4,7,10] Bridging forces in the asymmetric case would arise if the PEG chains had a preference to adsorb onto the opposing silicon substrate surface. However, in the present case, force−distance curves (data not shown) have shown that no adhesion is detected for either asymmetric or symmetric interfaces. This observation indicates that the bridging between PEG and bare SiO_2 colloidal probe and the entanglement of opposing polymer brushes can either be ruled out or are of minor importance. In line with the findings for the effect of the solvent quality, discussed previously in this paper, the differences in the friction forces for the asymmetric and symmetric tribointerfaces may rather be explained by differences in both the fluidity and the shear mobility of the brush interfaces. Notably, and as shown by Brown,[47] the shear stress associated with the brushes depends crucially on the segment mobility of the materials on both sides, and when the materials on both sides of the interface are highly mobile, as is the case in the brush−brush interaction (symmetric tribopair), lower stress is produced.

However, considering that the silicon wafer and the SiO_2 colloidal probe possess a finite surface roughness in the nanometer range, the interfacial film thickness is a potential parameter contributing to the differences in the coefficients of friction of the two tribosystems. Asperity contacts are less effectively shielded in the case of lower film thickness, and thus a higher additional shear force is likely to be required in the case of the asymmetrically coated tribointerface to overcome surface irregularities than for the symmetric tribopair.

In summary, we suggest that both the degree of interfacial fluidity and the polymer layer thickness play key roles in determining the lubrication performance of surface-bound brushlike polymers in general and of PLL-*g*-PEG in particular. Both solvent quality and the nature of the counterface can influence these parameters.

Conclusions

The friction forces between "symmetric" (both sides coated with PLL(20)-*g*[3.5]-PEG(5)) and "asymmetric" (Si wafer coated with PLL(20)-*g*[3.5]-PEG(5), silica probe unmodified) interfaces have been measured by means of colloidal probe LFM in relation to the mass of solvent absorbed in the unperturbed brushlike structure of the PEG chains. The mass of solvent absorbed in the PEG brush per unit area, referred to as solvation, was varied by choosing different solvents. The solvent environment plays a key role in determining both the conformational and the frictional properties of surface-bound brushlike polymers. Notably, both solvation and the coefficient of friction are strongly dependent on the nature of the solvent, characterized in terms of the three-component Hansen solubility parameters. It was found that solvation of the PEG brush decreases with both decreasing polar and decreasing hydrogen-bonding solubility parameters causing an increase of the coefficient of friction. No dependency of friction on the dispersion parameter was observed. The energy-dissipating components of the molecular interaction mechanism of surface-bound PLL-*g*-PEG have been discussed on the basis of the comparison of the frictional behavior of symmetric vs asymmetric coated tribointerfaces. In line with previous theoretical and experimental work, we conclude that both the interfacial fluidity and the segment mobility of the brush chains play a prominent role in determining the lubrication properties of brushlike polymers. Additionally, in cases where the substrate surfaces are not atomically smooth, a finite surface roughness may contribute to the observed tribological properties.

Acknowledgment. This work was financially supported by the Council of the Swiss Federal Institutes of Technology (ETH-Rat TopNano 21) and the US Air Force Office of Scientific Research (Contract F49620-02-1-0346). We are grateful to Dr. Janos Vörös of the Laboratory of Surface Science and Technology, ETH Zürich, Switzerland, for his valuable advice and assistance in the QCM-D and OWLS experiments.

References and Notes

(1) Klein, J.; Kumacheva, E.; Mahalu, D.; Perahia, D.; Fetters, L. J. *Nature (London)* **1994**, *370*, 634−636.

(2) Tadmor, R.; Janik, J.; Klein, J.; Fetters, L. J. *Phys. Rev. Lett.* **2003**, *91*, art. no.-115503.
(3) Raviv, U.; Tadmor, R.; Klein, J. *J. Phys. Chem. B* **2001**, *105*, 8125−8134.
(4) Klein, J.; Kumacheva, E.; Perahia, D.; Mahalu, D.; Warburg, S. *Faraday Discuss.* **1994**, *98*, 173−188.
(5) Fredrickson, G. H.; Pincus, P. *Langmuir* **1991**, *7*, 786−795.
(6) Kreer, T.; Müser, M. H. *Wear* **2003**, *254*, 827−831.
(7) Grest, G. S. *Adv. Polym. Sci.* **1999**, *138*, 149−183.
(8) Grest, G. S. *Phys. Rev. Lett.* **1996**, *76*, 4979−4982.
(9) Kreer, T.; Binder, K.; Muser, M. H. *Langmuir* **2003**, *19*, 7551−7559.
(10) Kampf, N.; Gohy, J.-F.; Jerome, R.; Klein, J. *J. Polym. Sci., Part B: Polym. Phys.* **2005**, *43*, 193−204.
(11) Klein, J. *J. Annu. Rev. Mater. Sci.* **1996**, *26*, 581−612.
(12) Schorr, P. A.; Kwan, T. C. B.; Kilbey, S. M.; Shaqfeh, E. S. G.; Tirrell, M. *Macromolecules* **2003**, *36*, 389−398.
(13) Granick, S.; Kumar, S. K.; Amis, E. J.; Antonietti, M.; Balazs, A. C.; Chakraborty, A. K.; Grest, G. S.; Hawker, C.; Janmey, P.; Kramer, E. J.; Nuzzo, R.; Russell, T. P.; Safinya, C. R. *J. Polym. Sci., Part B: Polym. Phys.* **2003**, *41*, 2755−2793.
(14) Raviv, U.; Giasson, S.; Kampf, N.; Gohy, J.-F.; Jérôme, R.; Klein, J. *Nature (London)* **2003**, *425*, 163−165.
(15) Yan, X. P.; Perry, S. S.; Spencer, N. D.; Pasche, S.; De Paul, S. M.; Textor, M.; Lim, M. S. *Langmuir* **2004**, *20*, 423−428.
(16) Lai, P. Y.; Binder, K. *J. Chem. Phys.* **1992**, *97*, 586−595.
(17) Roters, A.; Schimmel, M.; Ruhe, J.; Johannsmann, D. *Langmuir* **1998**, *14*, 3999−4004.
(18) Harris, M. J. E. *Poly(ethylene glycol) Chemistry: Biomedical and Biomedical Applications;* Plenum Press: New York: 1992.
(19) Elbert, D. L.; Hubbell, J. A. *Chem. Biol.* **1998**, *5*, 177−183.
(20) Kenausis, G. L.; Vörös, J.; Elbert, D. L.; Huang, N. P.; Hofer, R.; Ruiz-Taylor, L.; Textor, M.; Hubbell, J. A.; Spencer, N. D. *J. Phys. Chem. B* **2000**, *104*, 3298−3309.
(21) Pasche, S.; De Paul, S. M.; Vörös, J.; Spencer, N. D.; Textor, M. *Langmuir* **2003**, *19*, 9216−9225.
(22) Wagner, M. S.; Pasche, S.; Castner, D. G.; Textor, M. *Anal. Chem.* **2004**, *76*, 1483−1492.
(23) Heuberger, M.; Drobek, T.; Vörös, J. *Langmuir* **2004**, *20*, 9445−9448.
(24) Lee, S.; Müller, M.; Ratoi-Salagean, M.; Vörös, J.; Pasche, S.; De Paul, S. M.; Spikes, H. A.; Textor, M.; Spencer, N. D. *Tribol. Lett.* **2003**, *15*, 231−239.
(25) Müller, M.; Lee, S.; Spikes, H. A.; Spencer, N. D. *Tribol. Lett.* **2003**, *15*, 395−405.
(26) Stalgren, J. J. R.; Eriksson, J.; Boschkova, K. *J. Colloid Interface Sci.* **2002**, *253*, 190−195.
(27) Craig, V. S. J.; Plunkett, M. *J. Colloid Interface Sci.* **2003**, *262*, 126−129.
(28) Kurrat, R.; Textor, M.; Ramsden, J. J.; Böni, P.; Spencer, N. D. *Rev. Sci. Instrum.* **1997**, *68*, 2172−2176.
(29) Vörös, J.; Ramsden, J. J.; Csúcs, G.; Szendrö, I.; De Paul, S. M.; Textor, M.; Spencer, N. D. *Biomaterials* **2002**, *23*, 3699−3710.
(30) Hansen, C. M. *Hansen Solubility Parameters: A User's Handbook*, CRC Press: Boca Raton, FL, 2000; pp 3−208.
(31) Huang, N. P.; Michel, R.; Vörös, J.; Textor, M.; Hofer, R.; Rossi, A.; Elbert, D. L.; Hubbell, J. A.; Spencer, N. D. *Langmuir* **2001**, *17*, 489−498.
(32) Defeijter, J. A.; Benjamins, J.; Veer, F. A. *Biopolymers* **1978**, *17*, 1759−1772.
(33) Rodahl, M.; Höök, F.; Krozer, A.; Brzezinski, P.; Kasemo, B. *Rev. Sci. Instrum.* **1995**, *66*, 3924−3927.
(34) Vörös, J. *Biophys. J.* **2004**, *87*, 553−561.
(35) Rodahl, M.; Kasemo, B. *Sens. Actuators, A* **1996**, *54*, 448−456.
(36) Voinova, M. V.; Rodahl, M.; Jonson, M.; Kasemo, B. *Phys. Scr.* **1999**, *59*, 391−396.
(37) Bandey, H. L.; Hillman, A. R.; Brown, M. J.; Martin, S. J. *Faraday Discuss.* **1997**, *107*, 105−121.
(38) Larsson, C.; Rodahl, M.; Höök, F. *Anal. Chem.* **2003**, *75*, 5080−5087.
(39) Lide, D. R. *Handbook of Chemistry and Physics*, 72nd ed.; CRC Press: London, 1992; pp 15.43−15.50.
(40) Ogletree, D. F.; Carpick, R. W.; Salmeron, M. *Rev. Sci. Instrum.* **1996**, *67*, 3298−3306.
(41) Varenberg, M.; Etsion, I.; Halperin, G. *Rev. Sci. Instrum.* **2003**, *74*, 3362−3367.
(42) Pasche, S.; Textor, M.; Meagher, L.; Spencer, N. D.; Griesser, H. J., submitted to *Langmuir*.
(43) Barton, A. F. M. *Handbook of Polymer-Liquid Interaction Parameters and Solubility Parameters*, 2nd ed.; CRC Press: Boca Raton, FL, 1991; pp 11−15.
(44) Zhao, L. Y.; Choi, P. *Polymer* **2004**, *45*, 1349−1356.
(45) Raviv, U.; Frey, J.; Sak, R.; Laurat, P.; Tadmor, R.; Klein, J. *Langmuir* **2002**, *18*, 7482−7495.
(46) Tasaki, K. *J. Am. Chem. Soc.* **1996**, *118*, 8459−8469.
(47) Brown, H. R. *Science* **1994**, *263*, 1411−1413.

MA0501545